# Rotational-Optical Model for Scattering of Neutrons*

D. M. CHASE† AND L. WILETS,‡ *Los Alamos Scientific Laboratory, University of California, Los Alamos, New Mexico*

AND

A. R. EDMONDS,§ *Institute for Theoretical Physics, Copenhagen, Denmark*

(Received February 14, 1958)

The scattering of neutrons by a deformed, rotating, even-even nucleus has been investigated with a diffuse-surfaced complex potential employed. Two essential approximations, for which justification is presented, are made: (1) Nuclear excitations corresponding to $I \geq 6$ are ignored. (2) In the expansion of the nuclear potential, $V(r,\theta') = \sum v_\lambda(r) P_\lambda(\cos\theta')$, terms with $\lambda \geq 4$ are omitted. Comparison with earlier calculations by other authors, employing a distorted-wave Born approximation and $\delta$-function interaction, indicates that the earlier work seriously overestimated direct excitation. At low energies ($\lesssim 1$ Mev), the excitation cross section given by the direct process is small compared with excitation through the compound nucleus, but the direct process may contribute significantly to the angular distribution due to its large anistropy. The relevance of this work to the measurements of the differential cross section for excitation of the $I=2$ first excited level of $U^{238}$ is discussed in some detail. The general features of the experimental variation of the strength function $\bar{\Gamma}_n{}^0/D$ and potential-scattering length $R'$ with mass number at low energy have been reproduced by a calculation with suitably varying deformation.

## I. INTRODUCTION

MANY important properties of nuclei in the regions $90 \lesssim N \lesssim 112$ and $88 \lesssim Z$,[1,2] and in a certain region of light elements ($Z \sim 13$),[3] are correlated by the strong-coupling unified model, which supposes that these nuclei and their associated average potential fields possess large equilibrium deformations.[4] These large deformations can have significant consequences for the scattering of nuclear particles. For example, the scattering and absorption of low-energy neutrons, as described by a complex-potential or optical model,[5] depend sensitively on deformation. Differential elastic scattering cross sections, transmission coefficients, and all other scattering and reaction characteristics commonly considered must be expected to depend on deformation to some extent.

The effects of deformation just mentioned do not refer explicitly to the collective motion which is associated with the nuclear shape. Strongly deformed nuclei exhibit rotational spectra; these spectra, according to the strong-coupling model, correspond to a rotation of the nuclear shape and represent a particularly simple type of excitation. This motion must be rather strongly coupled by the large deformation to the motion of particles scattered by such nuclei. A mechanism is thus present for direct excitation of rotational levels by inelastic scattering without formation of a compound nucleus. Excitation of these levels by formation and decay of a compound nucleus also contributes, of course.

It is of interest, then, to calculate neutron scattering cross sections on the basis of a model which employs a complex potential well as in the optical model but with appropriately nonspherical shape, and which incorporates also a rotational motion. In the present work, all couplings apart from that to the collective rotational motion are assumed to be adequately simulated through the imaginary part of the potential. Similarly, it should be borne in mind that the direct coupling discussed here has been simulated in previous optical-model calculations by optimal choices of values for the available parameters. The previous choices of parameters will not generally be the best values here.

In Sec. II the model is formulated explicitly. In Sec. III results of calculations of cross sections for direct rotational excitation are presented and compared with cross sections for excitation via the compound nucleus. The former contribution is found to attain a sizable fraction of the latter for incident energies $E \gtrsim 1.5$ Mev. Angular distributions for the direct excitation are highly anisotropic and generally asymmetric with respect to 90°. Calculations in Sec. III for the most part are performed for a target nucleus having parameters characteristic of $U^{238}$. In Sec. IV the model is applied more extensively and specifically to $U^{238}$. Particular attention is given to the angular distribution for inelastic scattering to the first excited level; the result computed for compound-nucleus formation followed by statistical decay to that level[6] does not agree well with the experimental cross section at the incident energy $E=0.55$ Mev, but the calculated direct contribution does not considerably improve agreement at this low energy. In Sec. V is considered low-energy scattering, which is describable in terms of (1) the strength function or ratio of average neutron width to average level spacing in the

* Work performed, in part, under the auspices of the U. S. Atomic Energy Commission.

† Now at TRG, Inc., 17 Union Square West, New York, New York.

‡ On leave of absence to the Institute for Advanced Study, Princeton, New Jersey.

§ Present address: London Computer Center, Ferranti Ltd., London, England.

[1] B. R. Mottelson and S. G. Nilsson, Phys. Rev. **99**, 1615 (1955).

[2] G. Scharff-Goldhaber, Phys. Rev. **103**, 837 (1956).

[3] Gove, Litherland, and Paul, Physica **22**, 1141 (1956); G. Rakavy, Nuclear Phys. **4**, 375 (1957).

[4] A. Bohr and B. R. Mottelson, Kgl. Danske Videnskab. Selskab, Mat.-fys. Medd. **27**, No. 16 (1953).

[5] Feshbach, Porter, and Weisskopf, Phys. Rev. **96**, 448 (1954).

[6] L. Wolfenstein, Phys. Rev. **82**, 690 (1951); W. Hauser and H. Feshbach, Phys. Rev. **87**, 366 (1952).

compound nucleus and (2) the potential-scattering length. The general features of the experimentally determined variation of these quantities with mass number are successfully reproduced. The results for the strength function constitute the principal instance of improvement in agreement between calculation and experiment reported in this paper.

## II. FORMULATION OF THE MODEL

### A. Specification of the Problem; Expressions for Cross Sections

The Hamiltonian for the interacting system of rotating target nucleus and incident neutron is taken to be

$$H=-(\hbar^2/2m)\nabla^2+T_{\rm rot}+V(r,\theta'), \tag{1}$$

in which $T_{\rm rot}$ is the rotational energy operator for the target, assumed to be of fixed axially symmetric shape; $(r,\theta',\varphi')$ are the coordinates of the neutron relative to the nuclear principal axes; and $V(r,\theta')$ is the (complex) potential representing the interaction of the neutron with the deformed target. Spin of the neutron, and hence spin-orbit coupling, are omitted.

The Schrödinger equation for the target may be written

$$T_{\rm rot}D_{MK}{}^I(\theta_i)=\frac{\hbar^2}{2\mathcal{I}}[I(I+1)-K^2]D_{MK}{}^I(\theta_i), \tag{2}$$

$I=0, 2, 4, \cdots$ (ground-state band, even-even target, $K=0$),

$I=K, K+1, K+2, \cdots$ (odd-$A$ or odd-odd target, $K\neq\frac{1}{2}$).

Here $D_{MK}{}^I$ is the usual (unnormalized) symmetric-top wave function corresponding to a state of angular momentum $I$ with projections $M$ and $K$, respectively, along a space-fixed $z$ axis (chosen in the direction of the incident neutron beam) and the nuclear symmetry axis[7]; $\theta_i$ are the Euler angles of a set of principal nuclear axes relative to the space-fixed set[8]; and $\mathcal{I}$ is the moment of inertia for the rotation. The neutron-induced rotational transitions in question connect states of different $I$ within a band of fixed intrinsic character and projection $K$. In the present work, we shall restrict ourselves to the case $K=0$ with initial target spin $I=0$ (i.e., to even-even targets), which limits significantly the number of possible entrance channels and the complication of the expressions to be calculated.

To put the Schrödinger equation for the coupled system in a form convenient for solution, one may expand the potential $V(r,\theta')$ as

$$V(r,\theta')=\sum_\lambda v_\lambda(r)P_\lambda(\cos\theta'), \tag{3}$$

in which, for a plane-reflectionally invariant shape $[V(r,\theta')=V(r,\ \pi-\theta')]$, the sum runs over only even values of $\lambda$. A deformation coordinate $\beta$ may be defined by assuming the potential to be of the form

$$V(r,\theta')=V(r-R(\theta')), \tag{4}$$

where

$$R(\theta')=R_0[1+\beta Y_{20}(\theta')], \tag{5}$$

in which the constant $R_0$ may be defined by $V(0,\theta')R_0=\int_0^\infty V(r,\theta')dr$ so as to be something like an average effective radius when the well is both deformed and diffuse. The expansion coefficient $v_\lambda(r)$ in (3), when expanded as a power series in the deformation parameter $\beta$, contains no terms of lower degree in $\beta$ than $\beta^{\lambda/2}$.

We now write the wave function corresponding to an incoming partial wave of orbital angular momentum $l$ with $z$ projection $m=0$ in the channel $I=0$:

$$\psi^l=\sum_{l'I'}r^{-1}u_{l'I'}{}^l(r)_{l'}\mathcal{Y}_{I'}{}^{l0}(\theta,\varphi,\theta_1,\theta_2), \tag{6}$$

where $\mathcal{Y}_{l'I'}{}^{l0}$ contains the entire angular dependence for both the neutron and the nucleus, and constitutes an eigenfunction of total angular momentum $l$, with projection 0, composed of angular momentum $I'$ and $l'$; explicitly,

$$\mathcal{Y}_{l'I'}{}^{l0}=\sum_m(l'I'm,\ -m\,|\,l0)Y_{l'm}(\theta,\varphi)Y_{I',-m}(\theta_1,\theta_2). \tag{7}$$

(We have employed here for the nuclear wave functions the suitably normalized

$$Y_{IM}(\theta_1,\theta_2)=[(2I+1)/4\pi]^{\frac{1}{2}}(-)^MD_{M0}{}^I(\theta_i).)$$

Substitution of (1), (2), (3), and (6) into the Schrödinger equation $H\psi^l=E\psi^l$ yields the following coupled set of differential equations for the $u_{l'I'}{}^l(r)$:

$$\left\{\frac{\hbar^2}{2m}\left[-\frac{d^2}{dr^2}+\frac{l'(l'+1)}{r^2}\right]+\frac{\hbar^2}{2\mathcal{I}}I'(I'+1)+v_0(r)-E\right\}u_{l'I'}{}^l(r)$$
$$+v_2(r)\sum_{l''I''}\langle l''I'';\,l\,|\,P_2(\cos\theta')\,|\,l'I';\,l\rangle u_{l''I''}{}^l(r)=0, \tag{8}$$

where the terms $\lambda\geqslant 4$ in (2) have been neglected, as will be discussed presently, and the matrix element $\langle|\ |\rangle$ is given by [9]

$$\langle l''I'';\,l\,|\,P_2(\cos\theta')\,|\,l'I';\,l\rangle=W(I''l''I'l';\,l2)(2I''+1)^{\frac{1}{2}}\times(2l''+1)^{\frac{1}{2}}(2I''00\,|\,I'0)(2l''00\,|\,l'0). \tag{9}$$

For $r$ greater than the maximum extent of the potential $V(r,\theta')$, the radial wave functions $u_{l'I'}{}^l(r)$ have the form

$$r^{-1}u_{l0}{}^l(r)=\eta_{l0}{}^lh_l{}^{(1)}(k_0r)+h_l{}^{(2)}(k_0r),$$
$$r^{-1}u_{l'I'}{}^l(r)=(k_0/k_{I'})^{\frac{1}{2}}\eta_{l'I'}{}^lh_{l'}{}^{(1)}(k_{I'}r),\quad (I'\neq 0), \tag{10}$$

[7] Strictly, one must include the wave function for individual particles of the target and symmetrize with respect to the sign of $K$; the results here, however, are unchanged.

[8] In the notation of H. Goldstein [*Classical Mechanics* (Addison-Wesley Press, Cambridge, 1950)], for example, $(\theta_1,\theta_2,\theta_3)=(\theta,\varphi,\psi)$. $\theta_1$, in particular, is the angle between the symmetry axis and the direction of the incident beam.

[9] G. Racah, Phys. Rev. **62**, 438 (1942), Eqs. (38), (45), (50), and (51).

where the $h_l^{(1)}$, $h_l^{(2)}$ are the usual outgoing and incoming spherical Hankel functions, respectively[10];

$$k_I=[(2m/\hbar^2)E-(m/\mathcal{I})I(I+1)]^{\frac{1}{2}}$$

is a channel wave number; and $\eta_{I'I'}{}^l$ for open channels $I'$ is identical with the coefficient $S_{I'l';0l}{}^l$ of the collision matrix as commonly defined.[11] Equations (10) serve also to specify the normalization of $\psi^l$.

Differential cross sections for shape elastic scattering ($I'=0$) and direct inelastic scattering with excitation of the $I'$ rotational level ($I'=2, 4, \cdots$) are given in terms of the $\eta$'s by

$$\frac{d\sigma_{I'}{}^{(\mathrm{rot})}}{d\Omega}(\theta)=\frac{1}{4k_0^2}\sum_{m'=-I'}^{I'}\sum_{L=0}^{\infty}\sum_{l'=0}^{\infty}\sum_{l''=0}^{\infty}(-)^{m'}A_{l'm'}{}^{I'*}\times A_{l''m'}{}^{I'}(l'l''00|L0)\times(l'l''m',-m'|L0)P_L(\cos\theta), \quad (11)$$

$$A_{l'm'}{}^{I'}=\sum_{l=|l'-I'|}^{l'+I'}i^{l-l'}(2l+1)^{\frac{1}{2}}(2l'+1)^{\frac{1}{2}}\times(l'I'm',-m'|l0)(\delta_{I'0}\delta_{l'l}-\eta_{l'I'}{}^l).$$

The corresponding integrated cross sections are

$$\sigma_{I'}{}^{(\mathrm{rot})}=\frac{\pi}{k_0^2}\sum_{l=0}^{\infty}\sum_{l'=0}^{\infty}(2l+1)|\delta_{I'0}\delta_{l'l}-\eta_{l'I'}{}^l|^2. \quad (12)$$

Finally, the cross section for compound-nucleus formation[6] is

$$\sigma^{(c)}=\frac{\pi}{k_0^2}\sum_{l=0}^{\infty}(2l+1)(1-\sum_{I'}\sum_{l'}|\eta_{l'I'}{}^l|^2), \quad (13)$$

in which the sums over $I'$, $l'$ run over all possible values. The sum of the direct rotational excitation cross sections, $\sigma_2{}^{(\mathrm{rot})}+\sigma_4{}^{(\mathrm{rot})}$, will be denoted by $\sigma^{(\mathrm{rot})}$, and similarly for the differential cross sections. The total reaction cross section, $\sigma^{(\mathrm{rot})}+\sigma^{(c)}=(\pi/k_0^2)\sum_l(2l+1)\times(1-|\eta_{l0}{}^l|^2)$, will be denoted by $\sigma^{(\mathrm{reac})}$.

### B. Discussion of Approximations

The following approximations are made:

(i) Target states with $I\geqslant 6$ are neglected [Eqs. (6), (8)]. Without this restriction, the calculations would become quite unwieldy.[12] An indication that this neglect introduces no great error is provided by the calculations of Margolis and Troubetzkoy[13] on zero-energy scattering by a spheroidal potential. These workers found that the ratio of average neutron width to level spacing, $\bar{\Gamma}_n/D$, is but little changed by omission of terms with $l'\geqslant 6$ (implying the same for $I'$ since, in the limit of zero energy, $l=0$ only).

(ii) Contributions to the potential expansion (3) from $\lambda\geqslant 4$ are neglected. Even for a deformed square well, these can be shown to be quite small, as is illustrated in Fig. 1 (solid curves). The functions $v_\lambda(r)$ oscillate for $\lambda\geqslant 4$, with the average values of the functions being zero.

For a diffuse potential, the region of falloff of $v_0$ is increased; $v_2$ spreads out, with the volume remaining approximately constant; the $v_\lambda(\lambda\geqslant 4)$ not only spread out but also decrease in magnitude. These are illustrated in Fig. 1 (dashed curves) for a nuclear potential which is a linear function of $r-R(\theta')$ (see below) with a 1 to 0 falloff distance $\Delta'$ equal to $0.95\beta R_0$.[14]

Another reason for ignoring the $\lambda\geqslant 4$ is that nuclei undoubtedly possess intrinsic deformations of order higher than quadrupole and these, being unknown, contribute to the $v_\lambda(\lambda\geqslant 4)$ in an unknown manner. Therefore, it is only consistent with our present state of knowledge to ignore the higher orders.

(iii) For convenience, the nuclear potential form (4) is assumed with $V(r-R)\equiv V(x)$ a linear function in

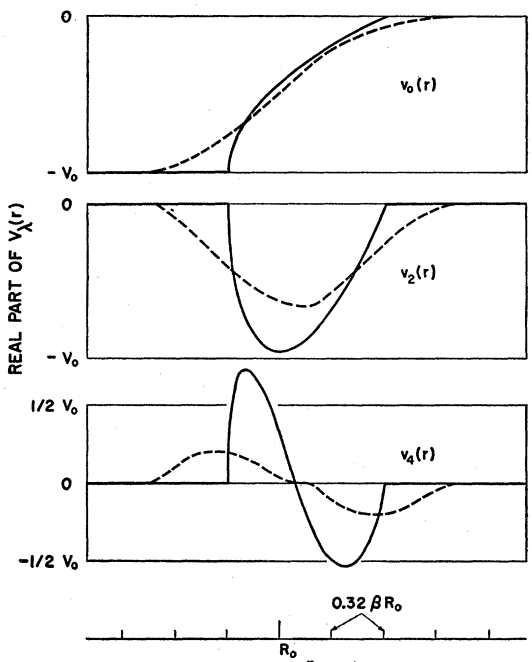


FIG. 1. Real part of radial potential functions $v_\lambda(r)$. The solid curves are for a deformed square well. The dashed curves are for a linearly diffuse potential of the type given in Eq. (14), with $\Delta'=0.95\beta R_0$.

[10] L. I. Schiff, *Quantum Mechanics* (McGraw-Hill Book Company, Inc., New York, 1949).

[11] J. M. Blatt and L. C. Biedenharn, Revs. Modern Phys. **24**, 258 (1952).

[12] States of higher spin could be included more easily in the adiabatic approximation [see D. M. Chase, Phys. Rev. **104**, 838 (1956); **106**, 516 (1957)], though their excitation energies would be neglected.

[13] B. Margolis and E. S. Troubetzkoy, Phys. Rev. **106**, 105 (1957).

[14] To terms of first order in $\beta$, $v_2(r)$ has the form of an inverted rectangle of width $\Delta'$ and area $(5/4\pi)^{\frac{1}{2}}V_0(1+i\zeta)R_0\beta$ independent of $\Delta'$ [see Eq. (21) below].

the surface region:

$$V(x)=-V_0(1+i\zeta)\times\begin{cases}1, & x\leqslant-\frac{1}{2}\Delta',\\ -x/\Delta'+\frac{1}{2}, & -\frac{1}{2}\Delta'<x<\frac{1}{2}\Delta',\\ 0, & \frac{1}{2}\Delta'\leqslant x.\end{cases}\quad(14)$$

The 90–10% falloff distance, $0.8\Delta'$, will be denoted by $\Delta$.

Early spherical optical-model calculations employed square-well potentials, while more recent investigations have employed various diffuse potentials, especially the so-called Saxon potential, which varies as $[1+e^{(r-R_0)/a}]^{-1}$. Present experimental data (and the model) are not sufficiently accurate to distinguish fine details of nuclear surface. The linear surface potential differs from the Saxon well in the appearance of corners, which can give rise to reflections resulting in small differences in angular distributions (see Sec. V). A linear surface potential *plus* deformation does not exhibit corners [see Fig. 1 (broken curves)].

For some of the earlier calculations reported here, $v_0(r)$ was further approximated by straight line segments and $v_2(r)$ by a parabola; results so obtained are specified accordingly.

### C. Incorporation of the Statistical Theory

As mentioned in Sec. I, excitation of rotational levels can occur *via* compound-nucleus formation as well as by direct excitation [for which the cross sections are given by (11) and (12) above]. Contributions of the former type will be computed by the statistical theory of Wolfenstein, and Hauser and Feshbach.[5] The statistical prescription originally given[5] requires generalization for the present sort of model, and this has already been given by Yoshida.[15] One may define an appropriate set of transmission coefficients, which in our case depend upon total angular momentum $J$, target spin $I$, and relative orbital angular momentum $l$ (as well as the channel wave number $k_I$): $T_{Il}{}^J(k_I)$. These are given explicitly as

$$T_{Il}{}^J=1-\sum_{I'}\sum_{l'}|S_{I'l';Il}{}^J|^2.\quad(15)$$

In computing the compound-nucleus contribution, one should take proper account of the intrinsic spin of the neutron, and therefore, though no spin-dependent interaction is included in the present work, it is convenient to employ transmission coefficients $T_{Isl}{}^J$ with a channel spin label $s$; $T_{Isl}{}^J$ is then given by Eq. (15) for both possible values, $I\pm\frac{1}{2}$, of $s$ ($s=\frac{1}{2}$ only, if $I=0$). In terms of the $T_{Isl}{}^J$, the differential cross section for excitation of the $I'$ level through compound-nucleus formation (from the $I=0$ ground state) is given by[16]

$$\frac{d\sigma_{I'}{}^{(c)}}{d\Omega}(\theta)=\frac{1}{k_0{}^2}\sum_{\lambda}B_{I'}{}^{\lambda}P_{\lambda}(\cos\theta),\quad(16)$$

$$B_{I'}{}^{\lambda}=\tfrac{1}{8}\sum_{s'}\sum_{l}\sum_{l'}\sum_{J}\frac{T_{0\frac{1}{2}l}{}^J(k_0)T_{I's'l'}{}^J(k_{I'})}{\sum_{I''s''l''}T_{I''s''l''}{}^J(k_{I''})}\times(-)^{s'-\frac{1}{2}}Z(lJlJ;\tfrac{1}{2}\lambda)Z(l'Jl'J;s'\lambda),\quad(17)$$

where $Z$ is as defined, for example, by Biedenharn, Blatt, and Rose.[17] The summation index $\lambda$ in (16) assumes only even values, thus giving an angular distribution symmetric about 90°, a well-known consequence of the neglect of interference terms in the statistical model. In the sums over $l'$, $l''$, and $I''$, proper account must be taken of conservation of parity. The corresponding integrated cross section is

$$\sigma_{I'}{}^{(c)}=\frac{\pi}{k_0{}^2}\tfrac{1}{2}\sum_{s'}\sum_{l}\sum_{l'}\sum_{J}\frac{(2J+1)T_{0\frac{1}{2}l}{}^J(k_0)T_{I's'l'}{}^J(k_{I'})}{\sum_{I''s''l''}T_{I''s''l''}{}^J(k_{I''})}.\quad(18)$$

[At energies above the threshold for excitation of states not belonging to the ground-state rotational band, such states should be included in the denominators of (17) and (18); this question lies outside the scope of the calculations to be described in this paper.] The entire excitation cross sections are to be obtained by simple addition of direct and compound-nucleus contributions, (11) and (16), (12) and (18).[18]

To calculate the required $T_{Il}{}^J$, one needs elements of the collision matrix other than $S_{I'l';0l}{}^l=\eta_{l'I'}{}^l$. These can be obtained similarly to the $\eta$'s by modifying suitably Eqs. (6), (8), and (10) to correspond to an incoming wave in channel $J$, $l$, $I$. Thus,

$$\psi^l\rightarrow\psi^{JlI},\quad u_{l'I'}{}^l(r)\rightarrow u_{l'I'}{}^{JlI}(r),$$
$$\langle l''I'';l|P_2|l'I';l\rangle\rightarrow\langle l''I'';J|P_2|l'I';J\rangle,$$

and Eqs. (10) become

$$r^{-1}u_{lI}{}^{JlI}(r)=S_{Il;Il}{}^Jh_l{}^{(1)}(k_Ir)+h_l{}^{(2)}(k_Ir),$$
$$r^{-1}u_{l'I'}{}^{JlI}(r)=(k_I/k_{I'})^{\frac{1}{2}}S_{I'l';Il}{}^Jh_l{}^{(1)}(k_{I'}r),\quad(I',l')\neq(I,l).\quad(19)$$

In the work to be reported in this paper, however, calculations have been made only with the entrance channel $I=0$ [as in (10)]; accordingly compound nucleus contributions have been computed by approximating the $T_{Il}{}^J$ in (16) and (18) (even those with $I=0$, apart from one hybrid calculation reported in Sec. V) by the $T_l$ computed for a spherically shaped potential.

[15] S. Yoshida, Proc. Phys. Soc. (London) **A69**, 668 (1956).

[16] For $I'=0$, expressions (16) and (18) represent compound elastic scattering.

[17] Biedenharn, Blatt, and Rose, Revs. Modern Phys. **24**, 249 (1952).

[18] The result satisfies the reciprocity theorem in consequence of the symmetry of the collision matrix $S_{I'l';Il}{}^J$. The latter retains its symmetry in spite of the complex potential and resultant non-Hermitian Hamiltonian because the Hamiltonian is symmetric. We are indebted to Dr. C. Longmire for elucidation of this point.

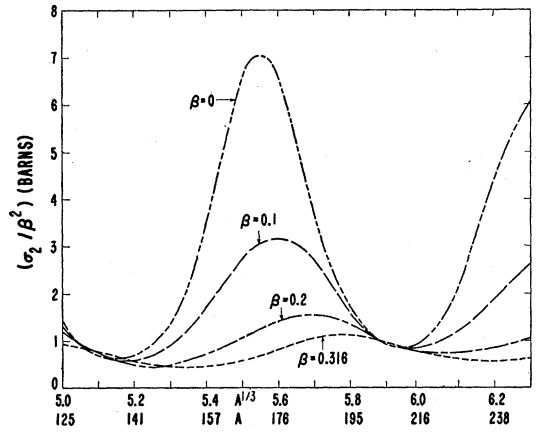


FIG. 2. Ratio of cross section $\sigma_2^{(\mathrm{rot})}$ for direct rotational excitation of the $I=2$ level to the square of the deformation parameter $\beta$, *vs* cube root of mass number $A$, for various values of $\beta$. The average radius $R_0$ of the deformed well is taken to be $r_0A^{\frac{1}{3}}$ with $r_0=1.35\times10^{-13}$ cm; other values assumed are diffuseness $\Delta=0$ (square well), well depth $V_0=42.2$ Mev, ratio of imaginary to real potential $\zeta=0.08$, energy of $I=2$ level $3\hbar^2/\mathcal{I}=50$ kev, and incident neutron energy $E=1$ Mev. If a distorted-wave Born approximation based on a $\delta$-function (linear-in-$\beta$) approximation to the extraspherical interaction were valid, curves would coincide independently of $\beta$; the lowering with increasing $\beta$ shows that such an approximation grossly overestimates $\sigma_2^{(\mathrm{rot})}$.

### D. Invalidity of the Distorted-Wave Born Approximation with δ-Function Interaction

Let us consider the distorted-wave Born approximation defined by employing a zero-order wave function obtained by omitting from the Hamiltonian the nonspherical terms

$$\sum_{\lambda\geq 2} v_\lambda(r)P_\lambda(\cos\theta') \qquad (20)$$

of $V(r,\theta')$ and then treating these in first order as a perturbation. [For the present discussion, (20) need not be cut off at $\lambda=2$.] This approximation gives cross sections correctly only to terms of no higher degree in $\beta$ than $\beta^2$, and accordingly is appropriate only for small deformation $\beta$. To the same order in $\beta$, all contributions from $\lambda>2$ in (20) vanish. The term $\lambda=2$ evidently connects the state $I=0$ only with $I'=2$ even if terms in $v_2(r)$ of arbitrarily high degree are retained. The part of the cross section $\sigma_2^{(\mathrm{rot})}$ of lowest degree in $\beta$ is proportional to $\beta^2$ and corresponds to retaining only the term in $v_2(r)$ of first degree in $\beta$. In the case of a square (nondiffuse) well, this term assumes the form given by

$$v_2(r)\rightarrow-(5/4\pi)^{\frac{1}{2}}V_0(1+i\zeta)R_0\beta\delta(r-R_0). \qquad (21)$$

To summarize, in the limit of small deformation ($\beta\rightarrow0$): (i) the above defined distorted-wave Born approximation for $d\sigma_2^{(\mathrm{rot})}/d\Omega$ and $\sigma_2^{(\mathrm{rot})}$ becomes correct to terms of the order of $\beta^2$; and (ii) if $V(r,\theta')$ is taken to be a square well, then, to terms of that same order in the cross sections, $v_2(r)$ may be replaced by the $\delta$-function surface interaction of (21). The first published results on this subject[19] were obtained by use of these approximations.[20] It is of interest to compare such results with those of the present more elaborate calculation.

One would expect approximation (ii) [Eq. (21)] to be adequate only if the maximum of $|R(\theta')-R_0|$, as given by (5), is much less than a quarter wavelength of the neutron in the neighborhood of $r=R_0$. Taking $\frac{1}{2}V_0$ for the local kinetic energy and inserting $\max|R(\theta')-R_0|=0.64\beta R_0$, one may express this condition as $(V_0/2D_0)^{\frac{1}{2}}(0.64\beta)\ll\pi/2$, where $D_0\equiv\hbar^2/2mR_0^2$, or $\beta\ll0.26$ for a heavy nucleus; this condition is not satisfied for the $\beta$'s of interest, which are $\simeq0.3$.

A distorted-wave Born approximation with a square well yields cross sections $\sigma_2^{(\mathrm{rot})}$, in the vicinity of a single-particle resonance, which for small enough absorption ($\zeta$) and reasonable $\beta$ may greatly exceed the maximum possible for conservation of particles. This result can be due only to use of the Born approximation [not to the interaction form (21)] and indicates that this approximation is unreliable for this problem.[21]

In Fig. 2 is shown $\sigma_2^{(\mathrm{rot})}/\beta^2$ as a function of the cube root of the mass number $A$ for various values of deformation $\beta$. Values of the other parameters are given in the caption. (This calculation is not directly applicable to actual nuclei because not all nuclei in the

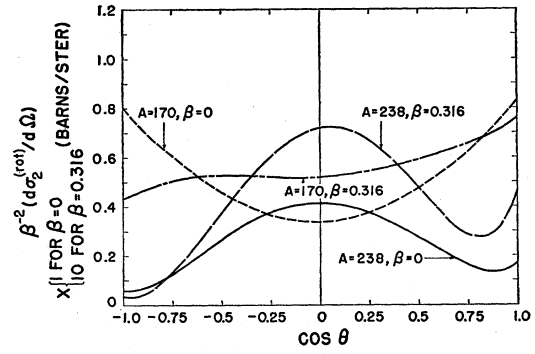


FIG. 3. Ratio of differential cross section $d\sigma_2^{(\mathrm{rot})}/d\Omega$ for excitation of the $I=2$ level to the square of the deformation $\beta$ for two values of $\beta$ at different $A$ (see Fig. 2). The curve for $\beta=0.316$ has been multiplied by a factor 10 relative to that for $\beta=0$ to render the shapes easily comparable. Results for $\beta=0$ represent those of a distorted-wave Born approximation with $\delta$-function surface interaction. Values of parameters are as given in the caption of Fig. 2. [The curves with $\beta\neq0$ and those of Fig. 2 were calculated with the special approximations to the potential functions $v_0(r)$ and $v_2(r)$ mentioned at the end of Sec. IIB.]

[19] D. M. Brink, Proc. Phys. Soc. (London) **A68**, 994 (1955); S. Hayakawa and S. Yoshida, Proc. Phys. Soc. (London) **A68**, 656 (1955); M. Moshinsky, Rev. Mex. Fis. **5**, 1 (1956).

[20] Results of the present machine calculation for $\sigma_2^{(\mathrm{rot})}$ as a function of $A$ in the limit of small $\beta$ with the parametric values used by Brink (see Fig. 2) do not quite agree with Brink's results, which were obtained in the distorted-wave approximation. Our curve is displaced toward lower $A$, to an extent somewhat dependent on $A$ and having higher peaks at the resonances relative to his. Accordingly, an independent distorted-wave Born approximation was made by machine; the results agreed substantially with our full-scale calculation. An earlier hand calculation also verified these results.

[21] See also Moshinsky (reference 19) and Yoshida (reference 15).

range exhibit a rotational spectrum and, moreover, $\hbar^2/2\mathcal{I}$ and $\beta$ are not independent of $A$.) If the Born and $\delta$-function approximation were valid, the curves for all $\beta$ would coincide with that labeled $\beta=0$. The absolute magnitude of $\sigma_2^{(\mathrm{rot})}/\beta^2$ at the single-particle resonances is seen from Fig. 3 to decrease by a factor $\sim 6$ from $\beta=0$ to $\beta=0.316$. Also, the resonance structure moves toward higher $A$; that is, the effective radius decreases with increasing $\beta$ for $R_0$ fixed and defined as it is here.

A similar calculation but with diffuseness $\Delta\simeq 3.0\times 10^{-13}$ cm gave a substantially larger $\sigma_2/\beta^2$ with a resonance structure displaced toward lower $A$.

In Fig. 3 are shown the corresponding differential cross sections $(d\sigma_2^{(\mathrm{rot})}/d\Omega)/\beta^2$ for $\beta=0$ and 0.316 at $A=170$ and 238. For $A=238$, the shapes (though, as just seen, not the magnitudes) for the two $\beta$'s are very similar, the anisotropy being somewhat larger, however, for the large $\beta$ than in the Born limit. For $A=170$, the shapes are considerably less similar, the anisotropy being somewhat less and the asymmetry relative to 90° greater for the large $\beta$. Since the single-particle resonance structure is shifted by changing $\beta$, one might expect most similar angular distributions for different $\beta$'s at different $A$; this did not prove to be true near the resonance peak at $A=170$ for $\beta=0$, and $A=191$ for $\beta=0.316$ (the result for the latter is not shown). The curves of Figs. 2 and 3 were calculated with the further approximation for $v_0(r)$ and $v_2(r)$ mentioned in Sec. IIB above.

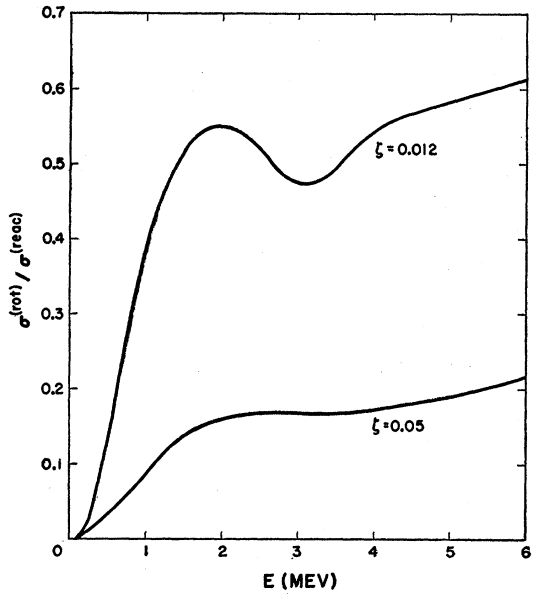


FIG. 4. Ratio of cross section for direct rotational excitation $\sigma^{(\mathrm{rot})}$ to total reaction cross section $\sigma^{(\mathrm{reac})}$ $(=\sigma^{(\mathrm{rot})}+\sigma^{(c)})$ for $U^{238}$ as a function of incident energy for two values of $\zeta$. Parameter values assumed are $R_0=1.35(238)^{\frac{1}{3}}\times 10^{-13}$ cm, $\Delta=2.2\times 10^{-13}$cm, $V_0=44$ Mev. The ratio attains a large fraction of its average value at an energy $E\sim 1$ Mev. The corresponding curve for $\zeta=0$ is a horizontal line at $\sigma^{(\mathrm{rot})}/\sigma^{(\mathrm{reac})}=1$ for $E>50$ kev. [These curves were computed with approximate expressions used for $v_0$ and $v_2$ (see text).]

## III. EXCITATION OF ROTATIONAL LEVELS WITH APPLICATION TO URANIUM-238

The uranium nucleus is strongly deformed and the naturally occurring element consists almost entirely of a single even-even isotope. Results of experimental measurements of its nonelastic, differential elastic, and total cross sections for neutrons are available,[22] and, in particular, measurements have recently been made by Cranberg and Levin[23] of the differential cross section at several angles for excitation of the $I=2$ rotational level. This nucleus, therefore, constitutes an auspicious case for investigation and application of the present model.

The present work must provide an answer to the essential question of how important is direct rotational interaction compared with compound-nucleus formation in determining cross sections. An indication of this is given in the discussion below.

Various calculations made with respect to $U^{238}$ show the general behavior of rotational excitation cross sections, including the effect of varying several parameters, and may be considered to apply qualitatively to other deformed nuclei. These results will be discussed here.

### *Direct vs Compound-Nucleus Excitation; Dependence on Imaginary Potential*

In Fig. 4 is plotted the calculated ratio of the direct rotational cross section $\sigma^{(\mathrm{rot})}$ to the total reaction cross section $\sigma^{(\mathrm{reac})}$ (including compound elastic scattering) as a function of incident energy $E$ for several values of the absorption parameter $\zeta$. Other parameters are those of the standard set.[24] The ratio depends rather sensitively on $\zeta$, being reduced by a factor $\sim 5$ for an increase of $\zeta$ from 0.012 to 0.05. The curves of Fig. 4 were calculated with the further approximation for $v_0$ and $v_2$ mentioned above, but the more exact calculation gives nearly the same result, especially for $\zeta=0.05$.

The predominance of the compound-nucleus contribution at low energy for inelastic scattering to the $I=2$ level alone may be seen in Fig. 5. The compound-nucleus part calculated in the WHF statistical theory, $\sigma_2^{(c)}$, for $\zeta=0.05$, and the direct part $\sigma_2^{(\mathrm{rot})}$, for $\zeta=0$ and 0.05, are given up to $E=0.55$ Mev (the energy of the Cranberg-Levin experiment[23]). ($\sigma_2^{(c)}$ was calculated from transmission coefficients of the spherical optical model with parameters approximating those given by Beyster and Walt[22] for $U^{238}$.) Evidently, at such energies, the direct rotational contribution is insignificant for the integrated cross section, but it will be seen below that it is not insignificant for the angular distribution because of its high anisotropy.

[22] M. Walt and J. R. Beyster, Los Alamos Scientific Laboratory Report LA-2061, 1956 (unpublished); Beyster, Walt, and Salmi, Phys. Rev. **104**, 1319 (1956).

[23] L. Cranberg and J. S. Levin, Phys. Rev. **109**, 2063 (1958).

[24] The set of parameters $r_0=1.35\times 10^{-13}$ cm, $\Delta=2.2\times 10^{-13}$ cm, $V_0=44$ Mev, $\zeta=0.012$, $\beta=0.33$, and $3\hbar^2/\mathcal{I}=50$ kev will be referred to conventionally as the standard set. $r_0$ is defined by the expression assumed for the average radius: $R_0=r_0A^{\frac{1}{3}}$. (The value $3\hbar^2/\mathcal{I}=45$ kev would be more nearly correct for the first excited state of $U^{238}$.)

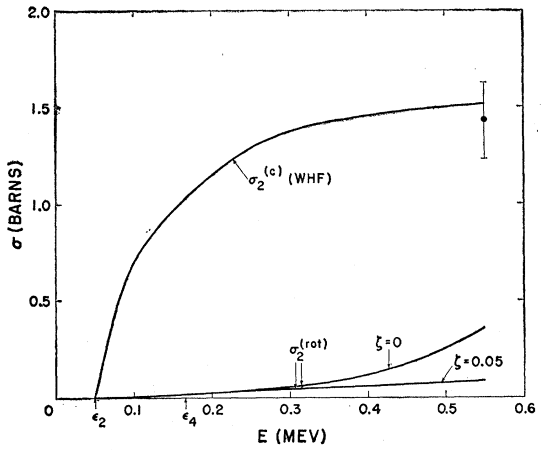


FIG. 5. Calculated partial excitation functions at low energy for the $I=2$ level of $U^{238}$. The curve labeled $\sigma_2^{(c)}$ represents the contribution from compound-nucleus formation according to the WHF statistical theory, and those labeled $\sigma_2^{(rot)}$ the contribution from direct rotational excitation. The former was calculated with $R_0=1.30(238)^{\frac{1}{3}}\times10^{-13}$ cm, $\Delta=2.0\times10^{-13}$ cm, $V_0=44$ Mev, $\zeta=0.05$, $\beta=0$, a set simulating the parameters determined in a spherical-well calculation for $U^{238}$ by Walt and Beyster[22]; the latter were calculated with $R_0=1.35(238)^{\frac{1}{3}}\times10^{-13}$ cm, $\Delta=2.2\times10^{-13}$ cm, $V_0=44$ Mev, $\beta=0.33$. A consistent calculation of $\sigma_2^{(c)}$ and $\sigma_2^{(rot)}$ would require use of Eq. (16) with transmission coefficients computed for the supposed $\beta$ of 0.33. In the low-energy range shown here, the slow-rising $\sigma_2^{(rot)}$ constitutes only a small fraction of the total $\sigma_2$. [The curves for $\sigma_2^{(rot)}$ were computed with approximate expressions used for $v_0$ and $v_2$ (see Sec. IIB).]

When the energy becomes so high that many channels are open, the statistical contribution $\sigma_2^{(c)}$ is expected to become very small compared with the calculated $\sigma_2^{(rot)}$. Thus, at sufficiently high energies ($\gtrsim10$ Mev), direct rotational excitation may predominate for the low-lying rotational levels exactly as direct particle excitation may for low-lying individual-particle levels.[25]

Also relevant to the present discussion is Fig. 6, where the direct excitation functions $\sigma_2^{(rot)}$ and $\sigma_4^{(rot)}$ are plotted up to $E=6$ Mev. With $\zeta=0$, these increase so steeply with energy above 0.5 Mev that both exceed the geometric cross section at $E\sim3$ Mev. The tremendous peak in $\sigma_4^{(rot)}$ at that energy is due largely to a resonance of the ingoing $l=4$ and outgoing $l'=4$ waves; the bump in $\sigma_2^{(rot)}$ at $E\sim1$ Mev results chiefly from $l=2$, $l'=0$ and $l=2$, $l'=2$ waves. As well as decreasing with increasing $\zeta$, the cross sections display a softer resonance structure, as would be expected. These calculations were made with use of the special approximation for $v_0$ and $v_2$, except that the result of an exact calculation is also shown for $\zeta=0.05$ only. The difference due to this change in $v_0$ and $v_2$ is seen to be very substantial for the quantities in question here.[26]

In order to determine at all closely the fractional contributions from direct rotational excitation, it is clearly necessary to establish the value of the parameter $\zeta$; or, conversely, the amount of direct excitation re-

TABLE I. Calculated cross sections $\sigma_2^{(rot)}$ and $\sigma_4^{(rot)}$ for direct excitation of $I=2$ and $I=4$ levels, and ratio $\sigma^{(rot)}/\sigma^{(reac)}$ of their sum to total reaction cross section, for $U^{238}$ and a typical even-even nucleus of the first rare-earth region at an incident energy $E=0.55$ Mev. The quantity $3\hbar^2/\mathcal{I}$ is equal to the energy assumed for the first excited ($I=2$) state. The diffuseness was inadvertently taken slightly different in the two cases, being $2.0\times10^{-13}$ cm for $A=180$ and $2.2\times10^{-13}$ cm for $A=238$. In these runs $\zeta$ was taken to have the small value of 0.012. These calculations were made with approximate expressions used for $v_0$ and $v_2$ (see Sec. IIB) and hence are subject to some uncertainty (see Fig. 6).

| $A$ | $3\hbar^2/\mathcal{I}$ (kev) | $\beta$ | $\sigma_2^{(rot)}$ (b) | $\sigma_4^{(rot)}$ (b) | $\sigma^{(reac)}$ (b) | $\sigma^{(rot)}/\sigma^{(reac)}$ |
|---|---|---|---|---|---|---|
| 180 | 90 | 0.30 | 0.66 | 0.016 | 2.15 | 0.314 |
| 238 | 50 | 0.33 | 0.18 | 0.024 | 1.29 | 0.159 |

[25] See S. T. Butler, Phys. Rev. **106**, 272 (1957). The necessary experimental measurements could presumably be made only with charged particles.

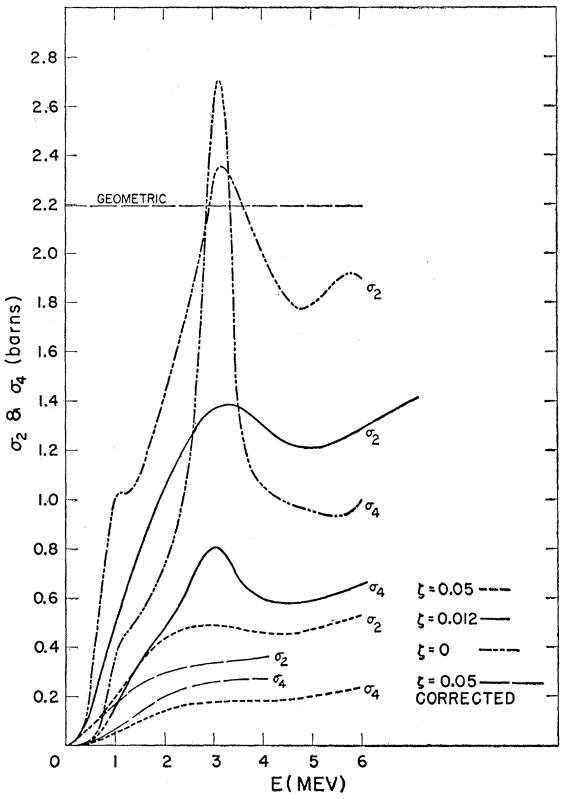


FIG. 6. Calculated excitation functions $\sigma_2^{(rot)}$ and $\sigma_4^{(rot)}$ for direct rotational excitation of the $I=2$ and $I=4$ levels of $U^{238}$ for various ratios of imaginary to real potential $\zeta$. Other parameters: $R_0=1.35(238)^{\frac{1}{3}}\times10^{-13}$ cm, $\Delta=2.2\times10^{-13}$ cm, $V_0=44$ Mev, $\beta=0.33$. Except for the curves labeled "corrected" (with $\zeta=0.05$), all curves were calculated by use of the approximate expressions for $v_0$ and $v_2$.

[26] The differential cross section $d\sigma_2^{(rot)}/d\Omega$ at $E=0.55$ Mev shown further on (Fig. 8) also is considerably different from that calculated from the approximation for $v_0$, $v_2$. The low-energy scattering quantities $\bar{\Gamma}_n/D$ and $R'$ (see Sec. VI), on the other hand, were not much affected. Sensitivity to the form of potentials may be slightly disturbing in view of the extent of the indeterminancy of the proper choice of spatial shape and radial variation and in view of the choice made here; however, the changes induced by altering $v_0$ and $v_2$ may only correspond to moderate but undetermined changes in the values of certain of the parameters, e.g., $r_0$.

quired for agreement with experimental inelastic angular distributions may determine $\zeta$ rather precisely.

*Comparative Results for First Rare-Earth Region*

A comparison will be interjected of the magnitude of direct rotational cross sections in the first rare-earth region with the magnitude for $U^{238}$, which was discussed above. This is summarized in Table I. Standard parameters[24] were used except for those listed, which are representative for the categories of nuclei in question; the energy $E$ is 0.55 Mev. The direct contribution $\sigma_2^{(\mathrm{rot})}$, it appears, may be considerably more important for even-even nuclei with $A\sim170$ than with $A\sim238$ (see Fig. 2).

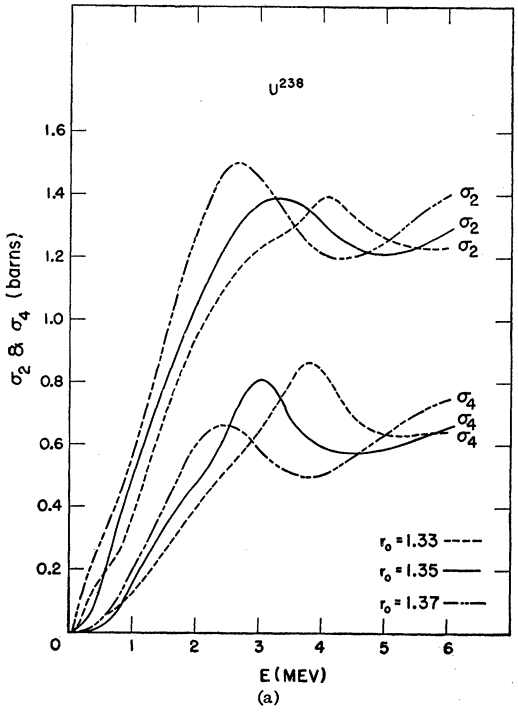


(a)

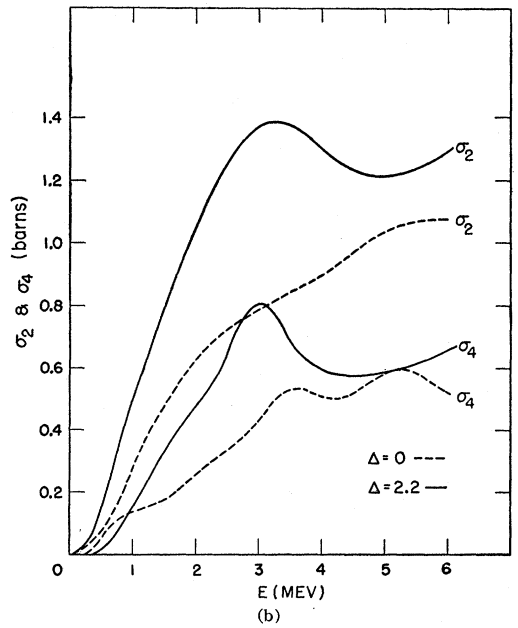


(b)

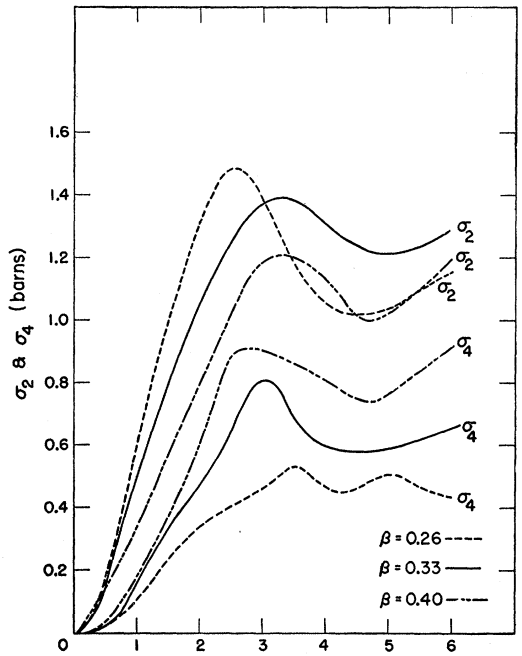


(c)

FIG. 7. Calculated excitation functions $\sigma_2^{(\mathrm{rot})}$ and $\sigma_4^{(\mathrm{rot})}$ of $U^{238}$ under variations of several parameters. The parameter varied in (a) is the average potential radius $R_0=r_0(238)^{\frac{1}{3}}\times10^{-13}$ cm, in (b), the diffuseness $\Delta$ (90–10% falloff distance), in (c), the deformation $\beta$. Parameters not otherwise specified are those of Fig. 6 with $\zeta=0.012$.

*Validity of the Adiabatic Approximation*

A calculation was made also with vanishing rotational level spacing (infinite moment of inertia $\mathcal{I}$) to test the validity of an adiabatic approximation.[12] The parameters assumed were those of Table I for $A=180$. (The particle energy of the adiabatic approximation was considered to be the average of the channel energies for initial and final states.) The error introduced in the direct rotational cross sections was less than 10% for energies a few hundred kev or more above threshold. Angular distributions displayed a greater difference but still were quite similar. These results indicate that this approximation would probably have sufficed for the present work. (If the states $I\gtrsim6$ were included, the deviation would likely increase slightly, to an extent dependent on the effect of these states on the calculated quantities.)

*Effect of Variation of Other Parameters*

The variation of the direct rotational cross sections with several of the parameters is discussed below. Except where specified, the parameters are those of the

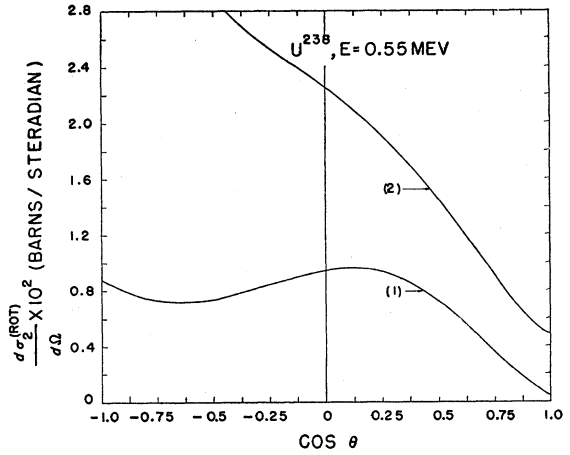


FIG. 8. Calculated differential cross section $d\sigma_2^{(\mathrm{rot})}/d\Omega$ for direct rotational excitation of the $I=2$ level of $U^{238}$ at an incident energy $E=0.55$ Mev. Parameters for curve (1) are those of Fig. 6 with $\zeta=0.05$; for (2), the same except $\zeta=0.012$ and $V_0=45$ Mev.

standard set.[24] Approximate expressions were used for $v_0$ and $v_2$.

*Variation with* $r_0$.—In Fig. 7(a) are shown $\sigma_2^{(\mathrm{rot})}$ and $\sigma_4^{(\mathrm{rot})}$, again up to an incident energy $E=6$ Mev, for three different values of the mean radius $R_0$ corresponding to $r_0=1.33$, 1.35, and 1.37, all $\times 10^{-13}$ cm. As would be expected, the single-particle resonance structure is shifted to lower energy by increasing $r_0$; the quantity $(V_0+E)r_0^2$, proportional to the square of the interior wave number, remains unchanged if $r_0$ is increased from 1.33 to 1.37 and $E$ decreased by $\sim 2.8$ Mev; the falloff toward threshold tends to reduce the shift of the maxima.

*Variation with* $\Delta$.—The effect of changing the diffuseness is indicated by Fig. 7(b), which gives $\sigma_2^{(\mathrm{rot})}$ and $\sigma_4^{(\mathrm{rot})}$ for $\Delta=0$ and $2.0\times 10^{-13}$ cm. These cross sections increase with diffuseness, as does $\sigma^{(e)}$; presumably this may be attributed to reduction of immediate elastic reflection.

*Variation with* $\beta$.—The *decrease* of $\sigma_2^{(\mathrm{rot})}$ with increasing $\beta$ (for $E<3$ Mev) constitutes an interesting feature in Fig. 7(c).

### *Angular Distributions*

A turn is made now to the differential cross sections $d\sigma_2^{(\mathrm{rot})}/d\Omega$ and $d\sigma_4^{(\mathrm{rot})}/d\Omega$. In Fig. 8 is shown the former of these at $E=0.55$ Mev with (2) the standard set of parameters, (1) the standard set except that $\zeta=0.05$. The salient characteristic is a strong anisotropy. For case (2) the distribution is strongly peaked rearward; for case (1) it is much reduced in the rearward hemisphere but still declines greatly in the forward direction. These curves will be discussed further in Sec. IV.

In Fig. 9 are given $d\sigma_2^{(\mathrm{rot})}/d\Omega$ and $d\sigma_4^{(\mathrm{rot})}/d\Omega$ at $E=2.5$ Mev with (1) the standard set of parameters and (2) the standard set except that $\zeta=0.05$. At this energy, the cross sections tend to peak between 0° and 90° and again between 90° and 180°; they are somewhat larger in the forward hemisphere. At a still higher energy, 4.1 Mev, the forward peaking is rather pronounced. Though the angular distributions are oscillatory, they bear yet little correspondence with the result of a plane-wave Born approximation using the $\delta$-function approximation (21); the Born distribution is given by the factor $[j_2(QR_0)]^2$, in which $Q$ is the momentum transfer $(k_I^2+k_{I'}^2-2k_Ik_{I'}\cos\theta)^{\frac{1}{2}}$.

## IV. SPECIFIC APPLICATION TO URANIUM-238

To effect a thorough study of a deformed nucleus with the present model requires determining suitable values for the parameters $r_0$, $\Delta$, $V_0$, $\zeta$, and $\beta$ (the energy of the first excited rotational state is presumed to be known). Except for $\beta$, all these parameters also enter the usual spherical optical model. As in the latter model, relevant experimental data include the differential elastic-scattering cross section, the nonelastic cross section, and (though not independent of these) the total cross section at various energies. In this optical-rotational model the differential and integrated partial cross sections for excitation of the $I=2$ and $I=4$ rotational levels are also of particular relevance.

Independent experimental and theoretical guidance may be looked to in choosing $r_0$, $\Delta$, $V_0$, and $\zeta$. Indications concerning $\Delta$ derive from high-energy electron scattering experiments. Fairly close estimates of $\beta$ have been made on the basis of measured ($E2$) transition probabilities between levels of a rotational band,[27] and by comparison of calculations of independent-particle states in a deformed well with observed properties of low-lying levels in strongly deformed nuclei.[28]

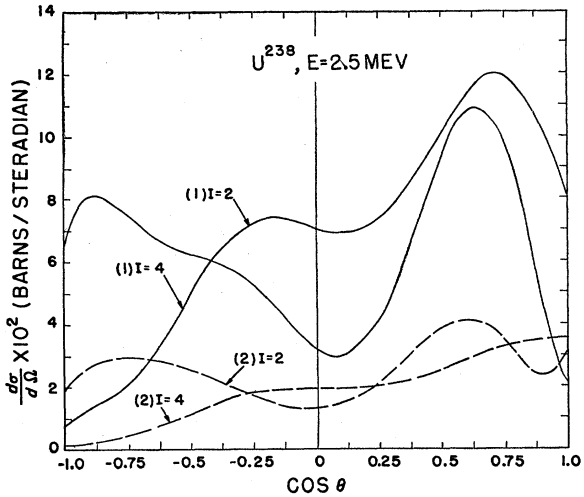


FIG. 9. Calculated differential cross sections $d\sigma_2^{(\mathrm{rot})}/d\Omega$ and $d\sigma_4^{(\mathrm{rot})}/d\Omega$ for $U^{238}$ at $E=2.5$ Mev. These are labeled $I=2$ and $I=4$, respectively. Parameters for curves (1) are those of Fig. 6 with $\zeta=0.012$; for (2), the same except $\zeta=0.05$.

[27] Alder, Bohr, Huus, Mottelson, and Winther, Revs. Modern Phys. **28**, 432 (1956); N. P. Heydenburg and G. M. Temmer, *Annual Review of Nuclear Science* (Annual Reviews, Inc., Stanford, 1956), Vol. 6, p. 77.

[28] B. R. Mottelson and S. G. Nilsson, Phys. Rev. **99**, 1615 (1955); S. G. Nilsson, Kgl. Danske Videnskab. Selskab, Mat.-fys. Medd. **29**, No. 16 (1955).

In the present work on $U^{238}$, a partial study has been carried out in the low-energy region ($E \lesssim 5$ Mev).

*Spherical limit; choice of* $\beta$.—It is appropriate to consider first how well the present calculation agrees, in the limit $\beta \to 0$, with previous spherical optical-model calculations, particularly in view of the employment here of a linear diffuseness. Figure 10 shows the total cross section $\sigma^{(tot)}$ and cross section for compound-nucleus formation $\sigma^{(c)}$ for $E<10$ Mev, calculated for $U^{238}$ by Beyster and Walt using a Saxon-type well, and the simulation thereto calculated in the present work with the same $r_0$, $V_0$, $\zeta$, and a diffuseness $\Delta=2.0\times10^{-13}$ cm, chosen to give approximately the best possible agreement for $\sigma^{(tot)}$ (a $\Delta$ of $2.2\times10^{-13}$ cm would give the same 90–10% falloff distance as that of Beyster and Walt). The agreement is rather good, the discrepancy being largest for 2 Mev$<E<$4 Mev, rather than at higher energy as one might expect from the consideration that the neutron would be better able to feel out the shape of the potential there. A comparison of the corresponding differential elastic cross sections at $E=2.5$ Mev is shown in Fig. 11. The agreement is good except in the valleys, where the potential with linear diffuseness yields deeper minima.

A choice for the value of nuclear deformation, $\beta$, must now be considered. A value of the intrinsic electric quadrupole moment of $U^{238}$ is available from Coulomb excitation.[27] This is a measure of the deformation of the nuclear charge distribution. It is an unsettled question whether the charge deformation is equal to the potential deformation—they are the same for an anisotropic harmonic oscillator at equilibrium (i.e., the energy is a minimum with respect to deformation for a given configuration). We have selected a value of $\beta=0.33$ for $U^{238}$ which represents an approximate mean between values reported from Coulomb excitation.[27] Our results are not sensitive to small variations in $\beta$.

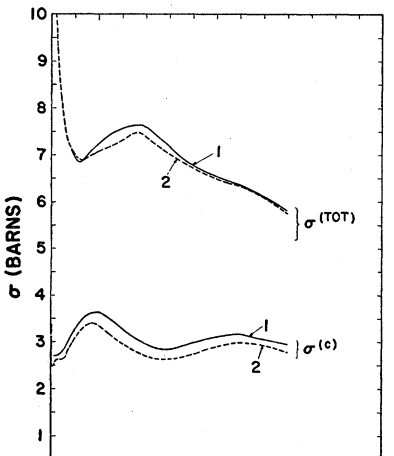


FIG. 10. Total and reaction cross sections for neutrons on $U^{238}$. Curves (1) represent the results of the spherical-well calculation of reference 22 (Saxon-type well, $r_0=1.30\times10^{-13}$ cm, 90–10% potential falloff distance$=2.2\times10^{-13}$ cm, $V_0$ decreasing from 44 Mev at low energies to 42.5 Mev at $E=10$ Mev, $\zeta$ increasing from 0.05 to 0.1). Curves (2) represent approximately the best simulation to the spherical-well computation which is obtainable with the linear falloff of Eq. (14) [90–10% falloff distance $\Delta=2.0\times10^{-13}$ cm, $r_0$, $V_0$, and $\zeta$ taken as in (1)].

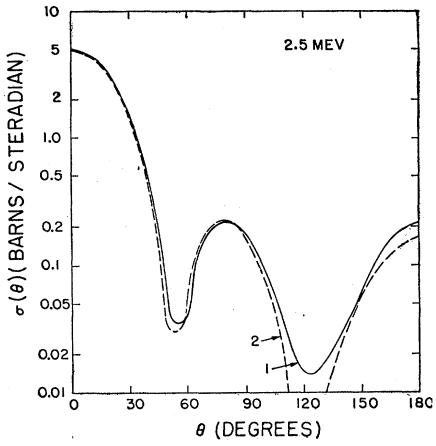


FIG. 11. Differential elastic-scattering cross sections for neutrons on $U^{238}$ at an incident energy $E=2.5$ Mev. The curves represent calculations of shape-elastic scattering: curves (1) and (2) are for the same parameters as (1) and (2) in Fig. 10.

*Total, reaction, and differential elastic cross sections.*—The total cross section was found to be approximately proportional to $R_0^2$ and independent of $V_0$ for variations in $V_0$ and $R_0$ which leave $(V_0+E)R^2$, i.e., the product of interior wave number and average radius, unchanged, a result which has been pointed out analytically in the spherical, square-well optical model.

A deep minimum in the total cross section around $E=1.5$ Mev represents a salient feature of the experimental data (in other heavy elements as well as $U^{238}$) and could be reproduced even very approximately only for quite limited ranges of several of the parameters. Favorable values of $V_0$ and $r_0$ lay in the neighborhood of 45 Mev and $1.35\times10^{-13}$ cm, but these values are somewhat uncertain since an adequate parameter study, using the correct expressions for the potential functions $v_0$ and $v_2$, was not carried out. To approach the desired minimum in $\sigma^{(tot)}$ appeared to require a very low absorption parameter ($\zeta\sim0.01$) at this energy.[29] (With $\beta=0$, on the other hand, a fair fit was achieved with $\zeta=0.075$.) Numerous considerations demonstrated, however, that such a low $\zeta$ is inappropriate for purposes of predicting and accounting for inelastic and reaction cross sections from the model. Specifically: (1) with $\zeta=0.012$ (and $r_0=1.35\times10^{-13}$ cm, $\Delta=2.2\times10^{-13}$ cm, $V^0=45$ Mev), at $E=0.55$ Mev (where the appropriate $\zeta$ would be expected to be at least as small as at 1.5 Mev) $\sigma^{(reac)}$ is computed to be 1.22 barns; the measurements of Cranberg and Levin[23] at this energy, however, yielded a larger value, 1.43

[29] A lower $\sigma^{(tot)}$ might be achieved by reducing $r_0$, according to the remark above, but the reduction required would be unreasonably large and presumably would not satisfy requirements at other energies.

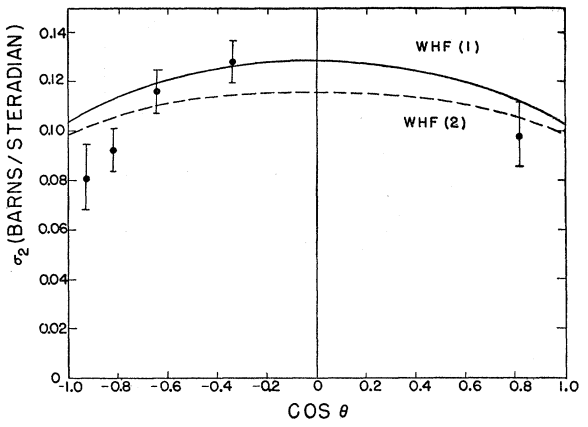


FIG. 12. Differential cross section for excitation of the $I=2$ level of $U^{238}$ at $E=0.55$ Mev. The experimental points are those of Cranberg and Levin.[23] The solid curve (1) is the cross section calculated on the basis of the WHF statistical theory, from transmission coefficients computed for a spherical well with parameters given in Fig. 5; the dashed curve (2) is a hybrid one calculated from the same outgoing transmission coefficients, but ingoing coefficients for a deformed well with the parameters of Fig. 6 and $\zeta=0.05$ (by use of the approximate forms of $v_0$ and $v_2$).

barns, for inelastic scattering to the $I=2$ level alone. (With $\zeta=0.05$ at 0.55 Mev one finds $\sigma^{(\text{reac})}=2.58$ barns.) (2) A very small $\zeta$ gives an angular distribution for scattering to the $I=2$ level which is contrary to experiment, as discussed below. (3) A very small $\zeta$ yields a ratio of average neutron width to level spacing at low energy, $\bar{\Gamma}_n^0/D$, of $0.41\times10^{-4}$ for $\zeta=0.012$ and $V_0=45$, a value much smaller than the measured one (see Sec. V).[30] (4) A value $\sim0.05$ for $\zeta$ accords with previous rough determinations of $\zeta$ for other (undeformed) nuclei from the spherical optical model.[31]

In connection with differential elastic cross sections, some difficulty was experienced in fitting the experimental maxima at $\theta\sim80°$ for $E=2.5$ Mev and, especially, 4.1 Mev. Since a thorough parameter study was not made, however, relevant curves are omitted. The spherical optical model, it may be mentioned, produced fairly satisfactory differential cross sections.[22]

*Differential inelastic cross section for the $I=2$ level.*—The experimental differential cross section for excitation of the $I=2$ first excited (45-kev) level of $U^{238}$ at an incident energy $E=0.55$ Mev, as measured by Cranberg and Levin,[23] is shown in Fig. 12. Shown also is the cross section $d\sigma_2^{(c)}/d\Omega$ calculated on the basis of the WHF statistical theory from (1) transmission coefficients computed, as in Fig. 5, for a spherical well, with $\zeta$, in particular, equal to 0.05, and (2) outgoing transmission coefficients computed for this same spherical well, but ingoing transmission coefficients [$T_{0l}{}^l(k_0)$ in Eq. (17)] computed for the deformed well with standard parameters[24] except $\zeta=0.05$ (hybrid). (The calculation of the $T_{0l}{}^l(k_0)$ was based on the approximate forms for $v_0$, $v_2$.)

The experimental results are substantially more anisotropic than those of the statistical calculations, and the difference is outside the estimated range of experimental uncertainty: the measured anisotropy defined by $\sigma(90°)-\sigma(157°)$ has a most probable value $\simeq55$ mb/sterad and a lower limit $\simeq41$ mb/sterad. The spherical-well statistical result is 25 mb/sterad. A consistent statistical calculation using transmission coefficients for the deformed well, on the other hand, might yield a somewhat different result. The hybrid calculation presumably provides some measure of this effect[32]; to the extent that it does, it seems unlikely that even a complete deformed-well computation would supply enough anisotropy for entirely satisfactory agreement between the compound-nucleus contribution and experiment.

The contribution from direct rotational excitation, $d\sigma_2^{(\text{rot})}/d\Omega$, was given for two sets of parameters in Fig. 10. The result for $\zeta=0.012$ is definitely excluded by experiment. The result for $\zeta=0.05$ is only slightly larger at $\theta=90°$ than at $\theta\sim157°$ and hence does not substantially help to account for the measured anisotropy. Increasing the well depth $V_0$ by 1 Mev or the diffuseness $\Delta$ by $0.3\times10^{-13}$ cm changed the angular distribution relatively little. (Parenthetically, a change leaving $V_0r_0^2$ unaltered produced virtually no effect.) Even if a distribution of the most favorable shape could be achieved by suitable changes in parameters, as may well be possible, the maximum effect is limited by the fact that at this energy the integrated cross section is relatively small if $\zeta$ is acceptably large ($\sim0.05$); specifically, it appears that $\sigma(90°)-\sigma(180°)$ cannot be larger than $\sim10$ mb/sterad for the direct contribution.

With regard to asymmetry relative to 90°, Cranberg and Levin measure $\sigma(35°)/\sigma(145°)=1.07\pm0.1$. From the lower limit, one finds $\sigma(145°)-\sigma(35°)<2.6$ mb/sterad. The WHF statistical theory, of course, yields no asymmetry. The direct contribution given by the curve of Fig. 8 for $\zeta=0.05$ is barely excluded by the lower limit (and that for $\zeta=0.012$ definitely so), but this circumstance could presumably be repaired by reasonable parameter juggling.

In summary, the observed anisotropy in excitation of the $I=2$ level is substantially larger than one would predict on the basis of the statistical theory with a spherical well and probably, though not certainly, also with the appropriate deformed well. Direct rotational excitation can supply at most about $\frac{1}{4}$ of the measured anisotropy [$\sigma(90°)-\sigma(157°)$].

Measurement of the angular correlation between the inelastically scattered neutron and the corresponding subsequent $\gamma$ ray might provide a means for dis-

[30] J. A. Harvey *et al.*, Phys. Rev. **99**, 10 (1955).
[31] J. R. Beyster and M. Walt, Los Alamos Scientific Laboratory Report LA-2099, 1957 (unpublished).
[32] Indicative, perhaps, of a potentially larger effect is the detailed result that transmission coefficients for $l=0$, 1, and 2 ingoing waves were changed from 0.25, 0.51, and 0.05, respectively, for the spherical well, to 0.48, 0.27, and 0.14 for the deformed well.

tinguishing more certainly the direct from the compound-nucleus contributions,[33] and constitute a sensitive indicator of satisfactory parameters.

With regard to neutrons of incident energy 2 Mev, the minimum $\simeq$90 mb/sterad at $\theta\simeq 60°$, obtained by Cranberg and Levin in the differential cross section for scattering to all levels below 0.5 Mev, imposes some restriction upon the allowable calculated $d\sigma_2^{(\mathrm{rot})}/d\Omega$ and $d\sigma_4^{(\mathrm{rot})}/d\Omega$ as well as upon the elastic contribution at this angle, and seems also to indicate that most of the compound-nucleus decay proceeds to higher levels. A computation at $E=2$ Mev with the standard parameters except that $\zeta=0.05$, for example, gives $d\sigma_2^{(\mathrm{rot})}/d\Omega=31$ mb/sterad, $d\sigma_4^{(\mathrm{rot})}/d\Omega=20$, $d\sigma_0^{(\mathrm{rot})}/d\Omega$ (shape elastic)$=91$ (which, however, is sensitive to the parameter values), all at $\theta=60°$, and $\sigma^{(c)}/4\pi=238$ mb/sterad.

## V. ZERO-ENERGY SCATTERING

The average low-energy reaction (or compound-nucleus formation) cross section can be related to the independently observed ratio of average neutron width, $\bar{\Gamma}_n$, to average level spacing, $D$, in the compound nucleus[34]:

$$\sigma^{(c)}=\sigma^{(\mathrm{reac})}=\frac{\pi}{k^2}(1-|\eta_{00}{}^0|^2)\simeq\frac{2\pi^2}{k^2}\frac{\bar{\Gamma}_n}{D}, \qquad (22)$$

according to Eq. (13). The potential elastic scattering cross section $\sigma^{(\mathrm{pe})}$ approaches a constant value at zero energy, which can be used to define a quantity $R'$ as the radius of a hard sphere yielding the same elastic cross section. Then in the neighborhood of zero energy

$$\sigma^{(\mathrm{pe})}=\sigma_0{}^{(\mathrm{rot})}=\frac{\pi}{k^2}|1-\eta_{00}{}^0|^2\simeq 4\pi R'^2, \qquad (23)$$

according to Eq. (12). The equalities on the right-hand sides of (22) and (23) obtain in the limit of zero incident neutron energy and, in the case of (22), well-spaced resonances.[6]

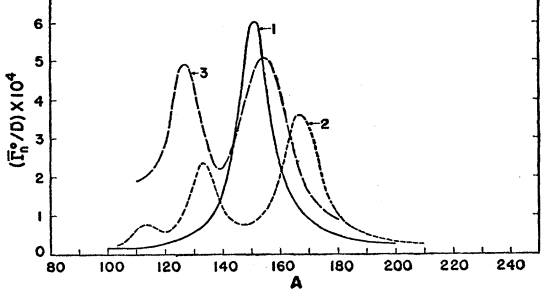


FIG. 13. Theoretical values of $\bar{\Gamma}_n{}^0/D$ (normalized to 1 ev) according to various nuclear models: (1) Spherical square well with $r_0=1.45\times10^{-13}$ cm, $V_0=42$ Mev, $\zeta=0.03$. (2) Spheroidal square well with same parameters as curve (1) and $\beta=0.150$, $3\hbar^2/\mathcal{I}=90$ kev. These are the same parameters employed by Margolis and Troubetzkoy[13] except that their $3\hbar^2/\mathcal{I}=0$; this curve is in agreement with theirs. (3) Diffuse spheroidal well with same parameters as (2) except $\Delta=2.5\times10^{-13}$ cm.

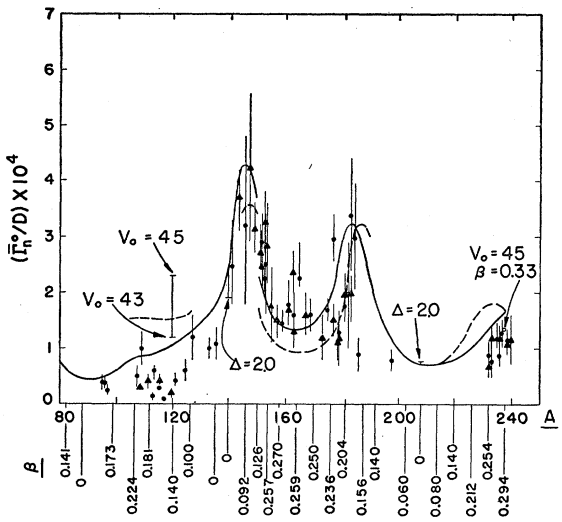


FIG. 14. Neutron strength function $\bar{\Gamma}_n{}^0/D$ as a function of mass number. $\bar{\Gamma}_n{}^0/D$ is the ratio of average $s$-wave neutron width to level spacing at low energy normalized to 1 ev. Experimental values are those of Zimmerman, Schwartz, and Hughes[36]; triangles indicate points from measurements on individual resonances, circles points from measurements of average cross sections in the kev region. The curves represent theoretical calculations based on a diffuse deformed complex-potential well. For the solid curve the variable deformation $\beta$ assumed is given at intervals in $A$ by the staggered numbers directly below the corresponding abscissas. Other parameters were assigned the fixed values $r_0=1.35\times10^{-13}$ cm, $\Delta=2.2\times10^{-13}$ cm, $V_0=44$ Mev, $\zeta=0.05$. The energy of the first excited level was varied appropriately with $A$. The dashed curve (where shown) was computed like the solid one but with a deformation larger by 33% at each point. At several values of $A$, the effect of varying a parameter is shown by a labeled point joined vertically with the appropriate curve. The sets of values of deformation were chosen primarily by reference to experimentally inferred intrinsic quadrupole moments.[27]

A spherical optical-model calculation for[35] $\bar{\Gamma}_n{}^0/D$ characteristically leads to a single maximum in the region $100<A<240$. With a deformed potential, the resonance splits, leading to two or more separated peaks. The splitting may be understood as arising from $l'=0$, 2, etc., resonances [see Eq. (8)].[13] The effect of deformation and diffuseness is illustrated in Fig. 13 for various parameters.

The curve for a deformed square well in Fig. 13 was calculated using the same parameters as Margolis and Troubetzkoy[13] and reproduces their results very well. This tends to confirm the validity of the adiabatic approximation (which they used) for $s$-wave scattering: the transit time of a neutron inside the nucleus is short compared with the period of nuclear rotation. The addition of diffuseness, however, increases the amplitude of the resonances.

Calculations of $\bar{\Gamma}_n{}^0/D$ were made also with the deformation varied with $A$ so as to agree with measured

[33] G. R. Satchler, Proc. Phys. Soc. (London) **A68**, 1037 (1955).
[34] See, for example, reference 6.
[35] The quantity $\bar{\Gamma}_n$ (and hence $\bar{\Gamma}_n/D$) is proportional to the incident wave number $k$. $\bar{\Gamma}_n{}^0$ represents $\bar{\Gamma}_n$ arbitrarily normalized to an incident energy $E=1$ ev.

TABLE II. Calculated strength function for $U^{238}$. The radius parameter $r_0$ was taken as $1.35\times10^{-13}$ cm and the deformation $\beta$ as 0.33 for each case.

| $\Delta$ ($10^{-13}$ cm) | $V_0$ (Mev) | $\zeta$ | $10^4\bar{\Gamma}_n^0/D$ |
|---|---|---|---|
| 2.2 | 44 | 0.05 | 1.60 |
| 2.2 | 45 | 0.012 | 0.42 |
| 2.2 | 45 | 0.05 | 1.33 |
| 2.5 | 44 | 0.05 | 1.50 |

intrinsic electric quadrupole moments.[27] The energies assumed for the first excited states similarly were varied roughly according to their observed average dependence on $A$. Other parameters were given fixed values considered generally appropriate on the basis of optical-model analyses of higher-energy scattering data; specifically, the values assumed were $\Delta=2.2\times10^{-13}$ cm, $r_0=1.35\times10^{-13}$ cm, and $V_0=44$ Mev and $\zeta=0.05$, except as otherwise noted. The calculated results and experimental measurements[36] are shown in Fig. 14. In certain intervals of $A$ the calculation was done for two sets of values of deformation, the larger values exceeding the smaller by 33%, corresponding roughly to the extent of experimental uncertainty[27] and indicating the degree of sensitivity to the values assumed. Similarly, at a few values of $A$ the effect of reasonable variations in the well depth $V_0$ and diffuseness $\Delta$ are displayed.

The general features of the experimental data are well reproduced by the calculation. Improvement over results of the spherical model due to splitting of the single-particle resonance at $A\simeq160$ is obtained as expected. The calculated $\bar{\Gamma}_n^0/D$ for the (strongly deformed) nuclei with $A\gtrsim230$ is as large as (indeed, for the parameters chosen, larger than) measured experimentally, a point of some previous question though a spherical potential with diffuseness may also achieve this result[37]; with large deformations a maximum even appears at $A\simeq230$ (Fig. 14).

Figure 14 shows that for many nuclei the calculated $\bar{\Gamma}_n^0/D$ is a rather sensitive function of some parameters of the model and, moreover, experimental values vary widely between neighboring elements. Accordingly, a more detailed program of fitting for specific nuclei, taking account also of other relevant scattering data, might profitably be undertaken. For $U^{238}$ the effect of variation of several parameters is displayed in Table II.

It has been assumed valid to compare results of the rotational-optical model, which, as formulated for the present calculations, properly applies only to even-even (spin-zero) targets, with measurements for nuclei of all types. By way of justification, it is pointed out that in the adiabatic approximation the scattering of $s$-waves by deformed nuclei is entirely independent of the spin of the target.

The potential-scattering length $R'$ corresponding to the calculation with variable $\beta$ is given in Fig. 15.[38] Shown also are (i) results of experimental measurements,[38] (ii) the strong-interaction model prediction, $R'=R$, and (iii) a prediction of the spherical optical model with diffuse surface.[39] The gross dependence on $A$, in so far as the experimental data determine it, is produced satisfactorily by both the deformed and the spherical optical-model curves. At a few points which pertain to substantially deformed nuclei, however, inclusion of an appropriate deformation appears to have improved the agreement appreciably. For tantalum the improvement is distinct, for samarium more marginal; for thorium improvement is attained only if the larger of the two assumed values of deformation is used. $R'$ is generally much less sensitive to variations in parameters than $\bar{\Gamma}_n^0/D$.

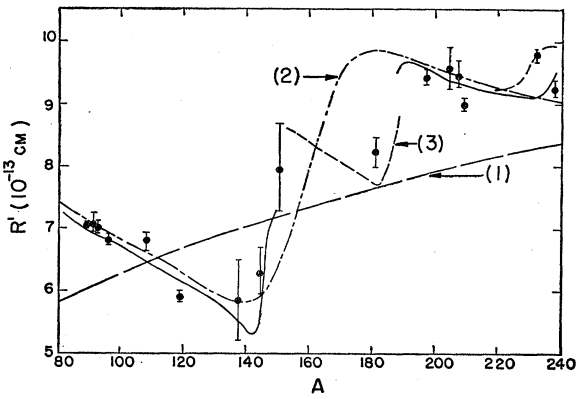


FIG. 15. Potential-scattering length $R'$ as a function of mass number. Experimental values are those of Seth, Hughes, and Zimmerman.[38] Solid and dashed curves (3) were computed from a deformed well as detailed for the corresponding curves in Fig. 14. (In intervals where both curves appear in Fig. 14 but only one here, the two curves differ little, and the one is shown which was determined more accurately. The apparent discontinuity at $A\simeq188$ is due to this procedure.) Curve (2), from reference 39, corresponds to a diffuse spherical well with $r_0=1.35\times10^{-13}$ cm, $V_0=42$ Mev, $\zeta=0.08$. Curve (1) corresponds to the strong-interaction model, being given by $R'=R=1.35A^{\frac{1}{3}}\times10^{-13}$ cm.

## VI. ACKNOWLEDGMENTS

The authors are greatly indebted to Mr. William Anderson for programming and executing the numerical calculations on the Los Alamos IBM-704 electronic computers. They wish to thank Dr. A. Bohr and Dr. B. R. Mottelson for valuable discussions.

Extensive consultation with Dr. L. Cranberg and Dr. J. Levin on experimental results and interpretation was invaluable and is gratefully acknowledged.

[36] Zimmerman, Schwartz, and Hughes, Bull. Am. Phys. Soc. Ser. II, 2, 218 (1957); R. M. Zimmerman, Proceedings of the Gatlinberg Conference on Neutron Physics by Time of Flight, 1956 [Oak Ridge National Laboratory Report ORNL-2309 (unpublished), p. 10].

[37] A small third-harmonic deformation of the nucleus also would affect $\bar{\Gamma}_n^0/D$ in this neighborhood [K. W. McVoy, Bull. Am. Phys. Soc. Ser. II, 3, 224 (1958)].

[38] Hughes, Seth, Zimmerman, and Garth, Phys. Rev. (to be published); K. K. Seth, Revs. Modern Phys. **30**, 442 (1958).

[39] Feshbach, Porter, and Campbell (unpublished); reported by V. F. Weisskopf in Physica **18**, 952 (1956).